Journal of Colloid and Interface Science **247,** 220–230 (2002)
doi:10.1006/jcis.2001.8100, available online at http://www.idealibrary.com on IDEAL®

The Relationship between Polymer/Substrate Charge Density and Charge Overcompensation by Adsorbed Polyelectrolyte Layers

Yongwoo Shin,* James E. Roberts,† and Maria M. Santore*,[1]

**Department of Chemical Engineering and †Department of Chemistry, Lehigh University, Bethlehem, Pennsylvania 18015*

Received July 31, 2001; accepted November 8, 2001

This work examines polyelectrolyte adsorption (exclusively driven by electrostatic attractions) for a model system (DMAEMA, polydimethylaminoethyl methacrylate, adsorbing onto silica) where the adsorbing polycation is more densely charged than the substrate. Variations in the relative charge densities of the polymer and substrate are accomplished by pH, and the polycation is of sufficiently low molecular weight that the adsorbed conformation is generally flat under all conditions examined. We demonstrate, quantitatively, that the charge overcompensation observed on the isotherm plateau can be attributed to the denser positive charge on the adsorbing polycation and that the ultimate coverage obtained corresponds to the adsorption of one oligomer onto each original negative silica charge, when the silica charge is most sparse, at pH 6. This limiting behavior breaks down at higher pHs where the greater silica charge density accommodates single chains adsorbing onto multiple negative sites. As a result of the greater substrate charge density and reduced polycation charge at higher pHs, the extent of charge overcompensation diminishes while the coverage increases on the plateau of the isotherm. Ultimately at the highest pHs, a regime is approached where the coil's excluded surface area, not surface charge, limits the ultimate coverage. In addition to quantifying the crossover from the charge-limiting to the area-limiting behaviors, this paper quantitatively reports adsorption-induced changes in bound counterion density and ionization at the interface, which were generally found to be independent of coverage for this model system. © 2002 Elsevier Science (USA)

Key Words: **polyelectrolyte adsorption; charge-limiting regime; geometry-limited regime; weak polyelectrolytes; counterions.**

INTRODUCTION

Certain cationic polyelectrolytes are employed extensively as flocculants in wastewater treatment and papermaking, while others form the basis for stabilizers or the anchoring groups of brush-forming copolymers. The right polyelectrolyte for a particular application depends on backbone chemistry, molecular architecture, charge density and placement, and interfacial dynamics, motivating a scientific focus on the interplay between these design features. The current work addresses the electrostatic aspects of charge-driven adsorption as a function of backbone charge density for a weak cationic polyelectrolyte adsorbing onto a weakly acidic surface, when the interfacial conformation is well-defined by the choice of a low-molecular-weight oligomer.

The most extensive studies of cationic polyelecrolyte adsorption have focused on quarternized systems, where permanently charged cationic units are not sensitive to pH (1–12). When adsorption is driven exclusively by electrostatic attractions, a threshold backbone charge density must be reached before the entropic loss of adsorption is overcome and significant mass accumulates at the interface (13–15). Greater amounts of backbone charge are, however, associated with lower coverages because increased backbone charge densities reduce the amount of polymer needed to compensate the underlying surface charge. These two effects, taken together, cause the surface coverage to exhibit a maximum with variations in backbone charge density (6, 16). An interesting observation is, however, that on the plateau of the isotherm, the surface charge is usually overcompensated (11, 12, 17–19). That is, more polymer adsorbs than is needed to neutralize the underlying surface charge. The reason for this overcompensation has been a source of speculation. For instance, it has been hypothesized that polymer-induced surface ionization drives further adsorption (1, 11, 17, 18).

In weak polyelectrolyte systems, the pH controls the underlying polymer charge. Additionally, for weakly acidic substrates such as silica, the surface charge is also pH-determined. When a weak polyelectrolyte adsorbs onto a weakly acidic surface, the pH in the interphase may differ from that in the bulk solution, such that the polymer and substrate charge densities are altered (20). Despite this complexity, coverage generally exhibits a maximum as pH is varied, a feature parallel to the influence of quarternized amine density in studies of strong polyelectrolyte adsorption (1, 21). It is therefore important, for weak polyelectrolytes, to understand the extent to which adsorption drives changes in polymer and surface ionization and if the mechanism more directly involves changes in local pH, dielectric properties, polymer conformation, or acid–base interactions. The altered polymer and surface ionizations must then be considered as potential driving forces for additional adsorption and charge overcompensation (1, 11, 17, 18).

[1] To whom correspondence should be addressed at Department of Polymer Science and Engineering, University of Massachusetts, Amherst, MA 01003.

0021-9797/02 $35.00

The situation is complicated by added ions, which can never be completely eliminated from fundamental studies and which are present at significant concentrations in most applications. Ions compete with the polyelectrolyte for adsorption sites on the surface, they screen the inter- and intrachain repulsions within an adsorbed layer, altering the chain conformations and the coverage (16, 22–24), and they contribute to counterion condensation on the polymer chain or the substrate when the underlying charge on either is relatively dense.

Counterion condensation has been all but neglected in most interpretations of experimentally measured polyelectrolyte adsorption (25). While it makes sense that counterions would condense to alleviate the energy associated with the close proximity of underlying charges on a polymer or surface, there are limited experimental reports of counterion condensation in polyelectrolyte solutions (26–28) or during polyelectrolyte adsorption (18). Counterion condensation is, however, extremely important. If counterions are released when a polyelectrolyte adheres to a surface, the entropy gain will further favor adsorption.

While mean field treatments typically applied to adsorption of nonionic polymers have been extended to polyelectrolyte adsorption (16, 20, 29), experimental evidence points to the necessity of a perspective involving localized charge densities. For instance, it has been observed that low-molecular-weight polyelectrolytes adsorbing onto oppositely charged surfaces induce flocculation of particles at very low surface coverages (9). This phenomenon, known as patchwise flocculation, occurs even though the adsorbing chains are relatively short and incapable of physically bridging between approaching particles (ruling out the mechanism of bridging flocculation). It is thought that the adsorption of certain polymers locally reverses the underlying surface charge (9, 12). Then, when only a small amount of such polymer is absorbed, the bare regions of the particle retain their original surface charge. As a result, each particle contains localized regions (patches) of positive and negative charges and flocculation occurs when oppositely charged regions on opposing particles attract.

Because of the potential for adsorbing polyelectrolytes to reverse the underlying surface charge at saturation or induce charge-related flocculation, we attempted to quantify the electrostatic features accompanying polyelectrolyte adsorption with a model system. To accomplish this we identified four related scientific issues:

1. How do pH and ionic strength affect the interfacial configuration and the amount of polymer bound to the surface in the form of trains?

2. To what extent are polycation protonation and substrate ionization in the adsorbed layer different from these properties for bulk solutions and bare silica, respectively, and to what extent are such differences influenced by bulk solution pH and ionic strength?

3. What is the role of counterion condensation in polyelectrolyte adsorption and can we detect any release of counterions on adsorption?

4. What is the mechanism by which charge overcompensation (adsorption of more cationic polymer than needed to neutralize negative charge, in the absence of purely chemical attractions) occurs?

The model system we employed to address these questions was a 15-unit oligomer of dimethylaminoethyl methacrylate (DMAEMA) whose adsorption on silica is exclusively driven by electrostatic attractions. In addition to the industrial importance of this weak polyelectrolyte as an anchoring block for dispersion stabilizers, the DMAEMA–silica system represents one limit of polyelectrolyte adsorption behavior: the polymer chains can be relatively densely charged at appropriately low pHs since each monomer can be protonated. In the pH range of interest, the underlying DMAEMA backbone charge density is greater than that on the silica. A second consequence of the high DMAEMA charge density is the substantial occurrence of counterion condensation (26, 30). Also the DMAEMA molecular weight is sufficiently low to render bridging flocculation unlikely and minimize the contributions of configurational entropy to the interfacial free energy (31). These properties are markedly different than those of strongly basic polyelectrolytes used as flocculants (and which have been the focus of much prior study). In the latter case, the molecular weights are high and the charge density on the backbone is often relatively low (3–11).

While all four of the afore-mentioned issues are intertwined, due to length constraints we addressed the first in a separate paper (21), while the others are the focus of the current work, using the same model system. The primary findings concerning coverage and interfacial conformation were that adsorbed DMAEMA layers were relatively flat, with many trains (80 wt% or more) and few loops and tails (21). Furthermore, the chain configuration was relatively insensitive to surface coverage for pHs from 6 to 8, the same range as the current work. The pH and, to a lesser extent, ionic strength was found, however, to influence the adsorbed conformation, with the highest bound fraction at a pH of 6 and low ionic strength. The influence of pH was thought to be related to the relative charge densities of the polymer and the substrate, motivating the current work.

In this paper, we employ NMR, titration, and electrophoretic mobility measurements to probe the electrostatic consequences of oligomer adsorption, summarized in questions 2–4.

EXPERIMENTAL METHODS

Materials. A 15-unit oligomer DMAEMA was provided as a gift from DuPont. The molecular weight was 2350 and the polydispersity was relatively low (1.1–1.3) as a result of the group transfer polymerization method. The DMAEMA sample was provided in a polar organic solution of isopropanol and tetrahyrdrofuran, which were replaced by D_2O in a rotary evaporator for NMR studies, until no solvent peaks were apparent in the NMR spectrum. For electrophoretic mobility and

titration experiments, the organic solvents were replaced, using a similar procedure, with high-purity distilled deionized (DDI) water (Milli-Q).

Monodisperse silica particles having a diameter of 200 nm were purchased from GelTech. These had a surface area of 15.7 m^2/g, as determined by the BET (Brunauer–Emmett–Teller) method on a Gemini 2360 surface area analyzer.

Buffering salts were purchased from Fischer Scientific and used as-received. Each buffer solution employed a 0.01 M solution of KH_2PO_4, to which sodium hydroxide was added. For instance, the pH 6 buffer consisted of 50 mL of KH_2PO_4 solution with 5.6 mL of 0.01 M NaOH added. The pH 7 and 8 buffer solutions employed 29.1 and 46.1 mL of NaOH solution, respectively.

Conductivity and pH. Titrations for DMAEMA protonation and silica ionization were based on conductivity and pH measurements. The former were carried out using a Yellow Spring Instrument (YSI Model 32) conductivity meter and a platinum immersion-type electrode (YSI Model 3403). The pH titrations employed a conventional glass electrode with a Corning Model 30 pH meter calibrated by pH 4.00 and 7.00 standards, from Fisher Scientific.

Electrophoretic mobility. Electrophoretic mobility studies employed a DELSA 440 instrument manufactured by the Coulter Company. A Coulter EMPSL7 mobility standard (carboxylated polystyrene latex in 0.1 M sodium phosphate buffer, pH 7.0) was employed for calibration.

Adsorption isotherms. The adsorbed amount present for a particular free DMAEMA solution concentration was determined by difference using solution-phase proton NMR. Typically, 5 wt% silica dispersions were employed, and the DMAEMA concentration was varied to generate an isotherm.

All NMR experiments were performed on a GN-300 300 MHz FT-NMR spectrometer, using a 10-mm proton/broadband probe. Samples containing silica, DMAEMA, and buffering salts were allowed to equilibrate for 10 min at room temperature before NMR measurements were made. The detailed features of the NMR data acquisition parameters were the same as those described in our previous paper (21). Of note, a benzene solution of tetrakis (trimethylsilyl) silane (TKS purchased from Aldrich) with added Chromium (III) acetonyl acetate was employed as an external standard in a sealed glass capillary tube. Also, a presaturation solvent suppression method (32) was applied to improve the dynamic range of the experiment.

RESULTS

Figure 1 presents the ionization and protonation, respectively, of the 200-nm silica particles and the DMAEMA oligomer at concentrations of 160 and 7800 ppm (1 and 50 meq/m^3). The ionization of the 200 nm particles, on the right axis, is quite similar to that of 12-nm Ludox silica particles employed in the adsorbed configuration study (21), except that the 200-nm particles

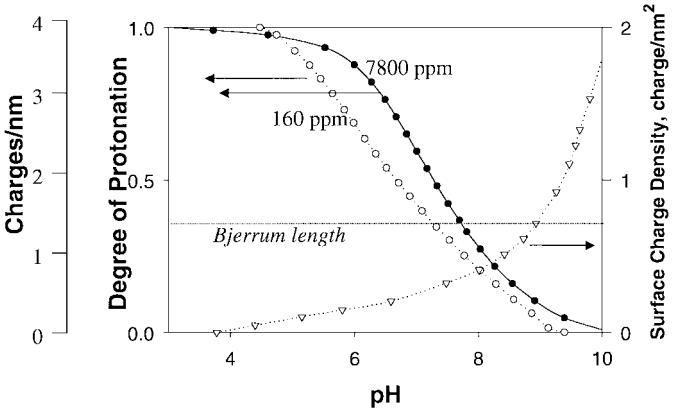

FIG. 1. Degree of DMAEMA protonation and silica surface charge density as a function of pH.

possess a slightly greater surface charge density. On the left axis, the DMAEMA protonation increases with decreasing pH, and a greater protonation extent is observed at higher DMAEMA concentrations. The charge spacing along the DMAEMA backbone, also on the left axis, was calculated by multiplying the fractional protonation from the titration results with 15 monomers/chain and then dividing by a contour length of 3.8 nm/chain. This charge density represents the average charge spacing along the backbone and neglects the detail that the charged amino groups reside on side chains, 0.6 nm from the backbone at full side-chain extension. Based on this method, the maximum underlying charge density of the DMAEMA is four charges/nm at low pHs.

Counterions are expected to condense on the DMAEMA chains when conditions are such that the underlying charge separation is less than the Bjerrum length, the intercharge distance corresponding to an energy of 1 kT (33, 34):

$$\lambda_b = \frac{e^2}{4\pi\varepsilon\varepsilon_0 kT}. \qquad [1]$$

Here, e is the elementary charge, and $\varepsilon\varepsilon_0$ is the dielectric constant of water.

For aqueous solutions the Bjerrum length is 0.7 nm. Counterion condensation on the DMAEMA would therefore be expected below pHs of 7.5, depending to a small degree on the polymer concentration, limiting the effective polycation charge to a maximum of 5.4 per chain. Indeed, conductimetric titrations have quantitatively confirmed this extensive counterion condensation (26, 30). True counterion condensation on the silica is not expected in the pH range of interest, since the underlying surface charge is relatively sparse, compared with λ_b. Cations may, however, bind to the silica surface with an increasing extent as the pH is increased above the isoelectric point of 3, as has been previously described (35, 36). Using previously reported equilibrium constants for sodium ion binding to negative silica sites and pHs of 6–8, we find that bound sodiums occupy no

more than 0.01, 0.1, and 1% of the negative surface sites (37). This amount of bound sodium is negligible, and with similar magnitudes of binding constants for potassium, a component of our buffer (35, 38), its binding would also be expected to be negligible.

One interesting feature borne out in Fig. 1 is that, over the range of pH 6–8 of interest in this study, the charge spacing on the DMAEMA backbone is denser than that on the silica surface. This is clearly the case when one examines the underlying positive charge on the polymer backbone, but it is also the case when one considers the net charge on the polymer, after counterion condensation. Only at pH 8 do the charge densities of the DMAEMA and silica begin to approach each other. This suggests that there will be regions of positive charge in the local vicinity of adsorbed DMAEMA chains unless the ionization of the polymer or surface are greatly altered by adsorption, or ion condensation is greatly altered by adsorption. We will explore this concept more quantitatively at a later stage of this work.

Figure 2 shows the adsorption isotherms for three different pHs, where adsorption was substantial. For each of the data sets in Fig. 2, the pH was controlled by adding 0.01 M NaOH and KH_2PO_4 to D_2O, with ionic strengths in the range 0.012–0.018 M. The nominal pHs shown in Fig. 2 pertain to the dilute regions of each isotherm. At coverages that were sufficiently large that the equilibrium concentration of DMAEMA in free solution was substantial, the bulk solution pH was roughly half a unit greater (near free solution concentrations of 2000 ppm) due to the basic nature of the DMAEMA.

The isotherms in Fig. 2 on the 200 nm GelTech silica particles are similar in shape and exhibit only slightly greater coverages compared with our prior results with 12-nm Ludox silica (21). The higher coverages on the GelTech particles presumably derive from their slightly greater surface charge density. At pH 6, there is a relatively flat pseudoplateau near 0.6 mg/m^2. At higher pHs the plateau region of the isotherm is more gradual, with coverages as high as 1.2 and 0.8 mg/m^2 for pHs of 8 and 7, respectively. The substantial adsorption in the intermediate pH range, where the silica is negatively charged and the DMAEMA

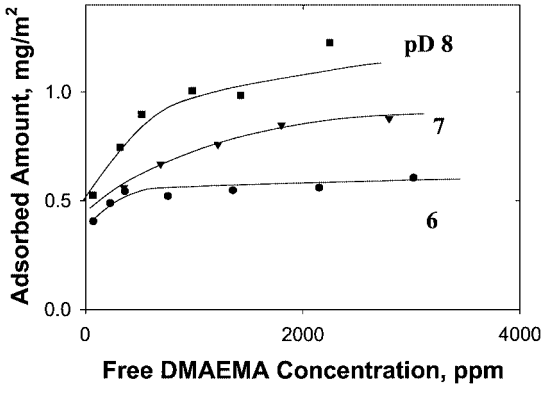

FIG. 2. Adsorption isotherms for DMAEMA on silica.

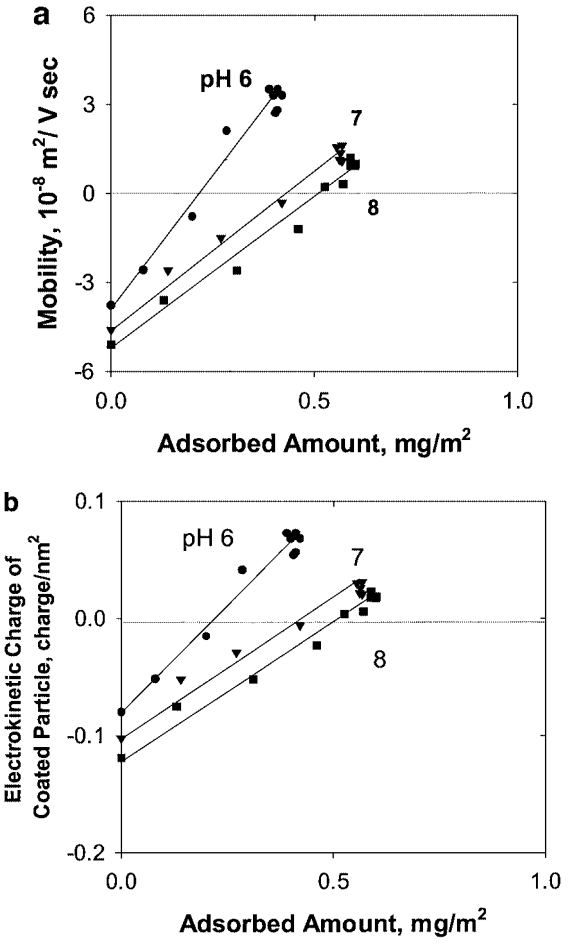

FIG. 3. (a) Electrophoretic mobility as a function of surface coverage. (b) Electrokinetic charge as a function of surface coverage.

is positively charged, suggests that the driving force for adsorption is electrostatic. The lack of adsorption (not shown here but previously documented in Refs. 21 and 37) at lowest and highest pHs additionally suggests that there is no chemical driving force for adsorption. The observation of a purely electrostatic driving force for DMAEMA on silica is similar to observations for its adsorption on TiO_2 (1).

Figure 3a presents electrophoretic mobilities related to the points on the isotherms in Fig. 2. (The mobility data were measured using silica concentrations that were 100 times more dilute than those of the isotherm measurements. The adsorbed amounts were inferred from Fig. 2, employing a mass balance.) In all cases, the adsorption caused an increase in the mobility, and at the highest surface coverages the mobilities are positive. This indicates that in the plateau regions of the isotherms, more polymer adsorbs than is needed to compensate the underlying negative silica charge. This overcompensation is most pronounced at a pH of 6 where the bare silica is relatively sparsely charged. Also, Fig. 3a reveals that, compared to the other pHs, less DMAEMA is needed to give the large overcompensation at pH 6.

In Fig. 3a at all three pHs, the electrophoretic mobility is linear in the adsorbed polymer, starting with the bare surface, and going well beyond the point of charge reversal. This suggests that, for a particular pH and ionic strength, each chain adsorbs in the same configuration, bringing the same net charge (including counterions) to the interface. There is no evidence that the first chains to adsorb on a bare surface are any different, from the electrostatic perspective, than those that adsorb near the point of charge neutralization or beyond. Further, Fig. 3 suggests that if the surface or polymer ionization is altered by polymer adsorption, this occurs to the same extent for each adsorbing chain. It is worth noting in Fig. 3a that the highest coverages obtained on the isotherms in Fig. 2 are not accessible in the mobility experiments due to the more dilute conditions required by the apparatus. The coverage axis in Fig. 3a does, however, span most of the isotherm.

Information about the net surface charge is contained within the electrophoretic mobility data. Typically, for particles substantially larger than the Debye layer thickness, $1/\kappa$, the Smoluchowski equation provides a relationship between the measured electrokinetic mobility, μ, and the zeta potential, ζ (39):

$$\mu = \frac{\varepsilon\zeta}{\eta}. \qquad [2a]$$

Here η is the viscosity of the solution, in this case water, and ε is its permittivity. The electrokinetic charge, σ_{EK}, then follows from the zeta potential, where the following expression applies to spherical particles of radius R:

$$\sigma_{EK} = \frac{\varepsilon(1+\kappa R)\zeta}{R}. \qquad [2b]$$

In addition to the net charge of the particle, which includes bound polymer and counterions, the electrokinetic charge also contains unbound ions inside the shear plane. For the bare silica particles, these are sodium or potassium ions that move with the particle, in addition to those which are chemically bound per site binding equilibria (35, 36). For the pHs in the current study, the reported site-binding constants for sodium and potassium ions are sufficiently small that bound cations contribute negligibly to the electrokinetic mobility (37). Rather, free ions inside the shear plane are more important.

Equation [2] applies to the limit when the particles are large compared with the Debye length. For the ionic strengths in the current study, the particle diameter was 33 times the Debye length; however, to ensure the most accurate determination of the electrokinetic mobility, we also applied the more exact expression summarized by Hunter (39), which approximates the full numerical solution of O'Brien and White (39–41). We find that for the current system, estimates of the electrokinetic charge by this method are indistinguishable from the predictions of the Smoluchowski equation.

A greater concern, perhaps, in the interpretation of the electrokinetic charge is the effect of adsorption on the position of the shear plane (42). The current work specifically focuses on a low-molecular-weight DMAEMA oligomer for this reason. We feel that with short chains that bind tightly to the surface, adsorption does little to alter the shear plane. This interpretation is upheld by NMR solvent relaxation experiments that indicate tight binding of the oligomer to the particle, independent of coverage, with most of the molecules (80% and usually more) lying flat as trains (21). With an overall chain length of 3.8 nm/oligomer, and tight binding, one might expect that the adsorbed DMAEMA would contribute at most a nanometer to the hydrodynamic particle size, avoiding measurable effects on the shear plane. This approximation is upheld by our dynamic light scattering data that detect no change in particle diameter on DMAEMA adsorption (37).

Figure 3b presents the electrokinetic charge from the mobility data from Fig. 3a. The linear forms in Fig. 3b uphold the conclusion that each oligomeric chain adsorbing at the interface, starting with the bare surface and including chains that adsorb well beyond the point of overcompensation, contributes the same electrokinetic charge to the particles, at a particular pH. That is, any change in the DMAEMA protonation, silica ionization, or number of counterions on the surface or associated with the DMAEMA is roughly independent of coverage. Further quantification, however, requires closer attention to the particle charge as a function of coverage.

The net surface charge is the sum of the negative underlying charge from the silica, the positive charge brought by the bound polymer, and counterions that adhere to the adsorbed polymer and also to the silica surface.

$$\text{Net surface chg} = \sigma_s + \sigma_{K+} + P_{\alpha+} + P_{C-}. \qquad [3]$$

Here, σ_s is the negative surface charge on the silica, σ_{K+} are the counterions (including both sodium and potassium) bound to the silica in the Helmholtz layer, $P_{\alpha+}$ is the underlying positive charge on the polymer, and P_{C-} are the counterions bound to the polymer, in this instance, phosphates (43).

Equation [3] is written for a particle bearing a layer of adsorbed polymer, and the four quantities on the right-hand side reflect the chemical physics of adsorption. For instance, the underlying surface charge, σ_s, may differ from that of the bare surface, σ_{so}. Here, σ_{so} is determined by titration (Fig. 1). Likewise in Eq. [3], $P_{\alpha+}$ and P_{C-} reflect the adsorbed DMAEMA, where chains in free solution may have different extents of ionization and amounts of bound counterions, $P_{\alpha+o}$ and P_{C-o}, respectively. It is actually $P_{\alpha+o}$ which is determined by the titrations in Fig. 1.

Equation [3] was initially written from the static perspective, counting charges that are chemically associated with the each particle, either through surface dissociation, polymer adsorption, or counterion (both K^+, Na^+ and phosphate) binding to the surface and/or polymer. The electrokinetic charge in Fig. 3b is more complex because it includes unbound ions inside the shear plane. For the bare silica particles, these are primarily sodium and potassium counterions; however, in the presence of

adsorbed polymer, the Na^+, K^+ and phosphate ions may be entrained to different extents. Hence, in applying Eq. [3], we recast our thinking to account for particle dynamics by including unbound cations within the shear plane in the σ_{C+} term, in addition to sodium and potassium ions which are chemically bound. The same potentially holds true for phosphate ions.

In the zero-coverage limit of Fig. 3b, the electrokinetic charge of the bare silica is much less than the titratable charge at the corresponding pH (Fig. 1). For instance, at pH 6, there is a net electrokinetic charge of $-0.08/nm^2$, while the titratable charge is $-0.16/nm^2$. This difference, $0.08/nm^2$, is attributed to sodium and potassium ions inside the shear plane in the electrophoretic mobility experiment, since our calculations using reported potassium and sodium binding constants indicate that true cation binding is negligible (37). At pH 7 and 8, the difference between electrokinetic and titratable charge suggests free cation contributions at densities of 0.15 and 0.25 charges/nm^2, respectively, inside the shear plane. This compares favorably with reports in the literature where titratable and electrokinetic charges on silica differed by ~50% (44, 45).

DISCUSSION

The previous section illustrated that (1) the silica surface ionization and DMAEMA protonation are pH dependent, with the DMAEMA being more densely charged than the silica over the pH range of interest, (2) the adsorption isotherms are pH dependent, most likely a result of the influence of pH on the silica and on the DMAEMA charge, (3) the net (electrokinetic) particle charge is linear in surface coverage for a wide range of surface coverages, and (4) the isotherm plateaus at all three pHs considered correspond to reversal of the underlying charge.

One additional piece of information, the size of the DMAEMA oligomer, is useful in developing perspective on the electrostatic nature of its adsorption. The DMAEMA oligomer's backbone contains 30 carbon atoms, leading to a chain length of 3.8 nm. Additionally, DMAEMA contains modest side chains, where the positive charge resides. The length of one side chain is 0.8 nm, such that if the DMAEMA adsorbs with its side chains on alternating sides of the main backbone, a maximum width of 1.6 nm could, in principle, be achieved. The dimensions 3.8×1.6 nm^2 yield the maximum footprint potentially occupied by adsorbed DMAEMA, and might occur under conditions where the backbone is highly charged. Counterion condensation will, however, reduce the extension of the backbone, and shift the conformation toward a random coil. Because the oligomeric chain is so short, it is unlikely that true Gaussian statistics would be achieved. However, if one estimates that 4 backbone carbons correspond to a statistical segment of length 0.5 nm, then a random coil size of 1 nm^2 is achieved based on πRg^2. If one alters this estimate to include six carbon atoms in a random segment with a length of 0.75 nm, then the footprint becomes 1.5 nm^2. In this manner we estimate each chain to occupy a surface area on the order of 1–2 nm^2.

Another measure of DMAEMA oligomer size includes the Debye screening length. At pH's of 6, 7, and 8, this length scale is 2.8, 2.5, and 2.2 nm, respectively. While the physical size of the chains is 1–2 nm^2, a Debye screening length of the same order means that adsorbed chains will repel each other before physical contact is made. Indeed, this repulsion should set in with 2–3 nm between adsorbed coils. Put another way, the excluded surface area per adsorbed chain would be in the range 5–10 nm^2, with smaller excluded surface areas at higher pH's.

Next we combine these facts to gain perspective on how adsorption can alter the surface polymer charge, including bound counterions. Also worth addressing is the mechanism for the reversal of surface charge. Many groups have previously reported overcompensation of surface charge for both quarternized and pH-dependent systems (1, 9, 11, 12, 17–19). Often, it was speculated that adsorption of cationic polymers causes the surface to further ionize, providing a driving force for overcompensation: the new negative surface charges generated drive the adsorption of even more cationic polymer, it has been said (1, 17). Here we examine the two effects individually, quantify their extents, and attempt to clarify which is cause and which is effect.

Ultimate Coverage and the Patchwise Adsorption Mechanism

It has been established that the driving force for DMAEMA adsorption on silica is electrostatic. Why then do the isotherm plateaus in Fig. 2 correspond to the adsorption of more polymer than is needed to neutralized the underlying surface charge?

The answer lies with an interfacial scenario that allows for localization of charge, in other words, a perspective that is not mean field. This situation is most pronounced at pH 6, where the plateau of the isotherm corresponds to the greatest of our three cases of charge overcompensation. Figure 1 illustrates that at pH 6, negative surface charges (on the bare surface), are widely separated by an average distance of 2.5 nm, or one charge/6.3 nm^2. This charge spacing modestly exceeds the DMAEMA size of 1–2 nm^2/chain, such that each oligomer, when it adsorbs, can interact with only one of the charges originally existing on the bare surface. Indeed, a maximum coverage of 0.60 mg/m^2 is predicted if one DMAEMA molecule adsorbs to each of the original negative charges on the bare silica. This simple calculation does an excellent job predicting the ultimate observed coverage, and strongly suggests that, at pH 6, single DMAEMA chains adsorb to single ionized surface silanols.

At pH 6, with single DMAEMA chains adsorbing to each of the original surface charges from the bare silica, the reversal of the underlying surface charge is then explained by the fact that each adsorbing chain brings with it more than one positive charge. As a result, in the vicinity of the adsorbing chain, there is a local positive charge. For situations where the surface is not yet saturated, regions containing no DMAEMA still exhibit their original negative charges, giving rise to a patchy interface, from the perspective of charge localization. The extent of overcompensation depends on the amounts of positive charge brought to

TABLE 1
Assessing Surface Charge as the Limiting Factor in the Plateau Coverage

pH	Bare surface charge ($1/\sigma_{so}$, nm^2/charge)	Expected coverage w/1 chain/surface charge (mg/m^2)	Observed coverage (mg/m^2)
6	6.3	0.6	0.60
7	3.3	1.2	0.80
8	1.9	2.0	1.2

the interface by the DMAEMA, an issue addressed in the next section of the discussion.

At pH 6, adsorption is patchy and individual DMAEMA chains adhere to isolated negative surface charges until all the ionized silanols from the bare surface each carry one DMAEMA chain. The situation is more complicated at pHs 7 and 8, because now the silica is more densely populated with negative charges. Thus, adsorbing DMAEMA chains are likely to encounter more than a single original negative charge. Indeed, if one attempts to predict the ultimate plateau coverage based on one chain per underlying surface charge (see Table 1), the calculated coverage exceeds that observed, especially at pH 8.

At pH 7 and 8, the breakdown of a one-chain-per-surface-charge adsorption mechanism suggests a crossover to a scenario which is more geometric. Since the surface is more densely charged, chains may access multiple charged surface sites, and therefore repulsions between neighboring chains must ultimately limit coverage. The surface may saturate when the backbones crowd the interface, or it may saturate when the surface is full in the electrostatic sense, i.e., when the excluded surface areas of the adsorbed oligomers fill the surface. Of note, at pH 8, the observed maximum plateau coverage of 1.2 mg/m^2 corresponds to a surface area of 3.4 nm^2/chain, which exceeds the DMAEMA's molecular dimensions. It is, however, smaller than the excluded area per chain, suggesting that lateral repulsions among adsorbed coils are significant and ultimately limit the coverage. Indeed the gradual plateau at pH 8 may result from soft electrostatic repulsions between neighboring adsorbed oligomers, as opposed to a more abrupt plateau, which might be expected if the adsorbing species exhibited hard lateral repulsions.

It is worth mentioning that we did witness additional evidence for patchy interfaces, from the perspective of localized charge. That is, once DMAEMA was adsorbed, the particles tended to flocculate, and it was necessary to operate at dilute conditions and perform experiments quickly (and check reproducibility) to avoid artifacts from flocculation. While flocculation may be expected at conditions yielding particles with nearly zero net charge, we observed flocculation over a broader range of conditions, where the surface charge should have been sufficient to stabilize the particles, if the interface had a constant spatially averaged charge instead of charge patches. While bare silica particles were stable, flocculation was observed for as little as 0.1 mg/m^2. This is attributed to patchwise flocculation since the DMAEMA oligomer is too short to bridge between approaching particles.

Ionization and Condensed Ions

In the previous section we argued that charge localization maintained a continued driving force for DMAEMA adsorption well beyond the point where the average interfacial charge was neutral. The release of counterions or any additional surface ionization was not required to drive the adsorption of additional DMAEMA beyond the point of net particle neutralization. Further, there was evidence for regions of positive charge in the vicinity of adsorbed polymer, coexisting with regions of negative charges in the vicinity of bare silica. It is therefore worth attempting to determine the local extent of overcharging in the region of adsorbed polymer and the extent of any changes in the numbers of bound Na^+, K^+, or phosphate ions, DMAEMA protonation, or silica ionization, resulting from adsorption.

To help visualize the interfacial physics, we consider a 5× 5-nm unit cell of the surface, as shown in Fig. 4a. At pH 6, this region contains four titratable negative surface charges, as determined in Fig. 1. From Fig. 3b, we additionally infer the presence of two unbound Na^+ or K^+ ions inside the shear plane. Likewise, at pHs 7 and 8 in Figs. 4b and 4c, the titratable surface charge increases to 7 and 13, respectively, while there are 4.2 and 8.8 unbound cations, respectively, inside the shear plane.

In the initial state, our system contains this bare silica unit cell with unbound cations inside the shear plane and the free DMAEMA with its bound phosphate counterions in solution. In Fig. 4, where the polymer is shown, only the net positive charge on the polymer is drawn. The details of the underlying titratable charge and the anion binding are eliminated to avoid crowding the drawing. In the final state, the polymer is adsorbed, with potential alterations in the surface ionization or DMAEMA protonation, and potential release of Na^+, K^+, or phosphate counterions.

We proceed with calculations based on coverages corresponding to the points of zero net mobility, in Fig. 3. For pH 6, this corresponds to a surface coverage of 0.22 mg/m^2, or 1.4 chains adsorbing in the 25 nm^2 unit cell. Prior to adsorption, when these chains were free in solution at pH 6, they each possessed an underlying charge of 10.2 /chain, but due to the condensation of 4.8 negative counterion charges per chain, they each carried a net charge of 5.4/chain (26, 30). The change in interfacial charge, for the entire unit cell as a result of adsorption is therefore

$$\begin{aligned}\Delta \text{ charge (per 25 nm}^2) &= 0 - (\sigma_{so} + \sigma_{K+o} + P_{\alpha+o} + P_{C-o}) \\ &= 0 - (-4 + 2 + 14.2 + -6.7) = -5.5.\end{aligned} \quad [4]$$

Here the final charge in the cell after adsorption was determined by the electrokinetic mobility, and is zero at the point of zero charge. The initial charges are known from the properties of the

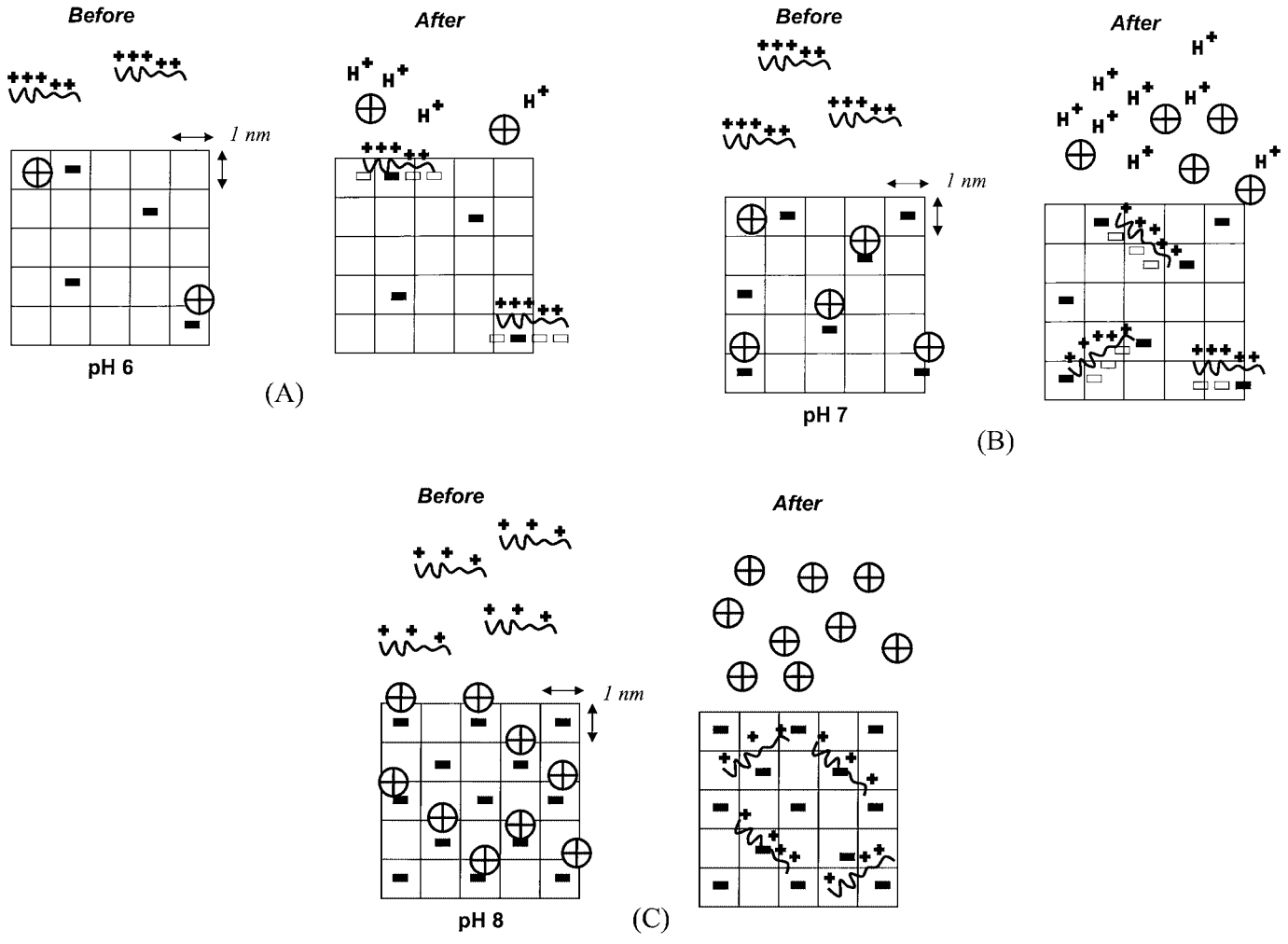

FIG. 4. Schematic of 25 nm^2 unit cell on silica surface before and after DMAEMA adsorption at (A) pH 6, (B) pH 7, and (C) pH 8. The "Before" state corresponds to the bare silica surface while the "After" state corresponds to one where there is no net electrokinetic charge on the particle. The black negative charges correspond to those originally present on the bare silica surface. The white (or hollow) negative charges correspond to those which ionize locally as a result of oligomer adhesion. The plus signs in the circles illustrate hydrodynamically entrained potassium and sodium ions, which are present near the surface initially but are displaced as a result of adsorption. The positive charges on the oligomer represent the net oligomer charge after binding of phosphate counterions to the backbone. Protons released as a result of the local surface ionization are shown explicitly in the "After" state.

free polymer in Fig. 1 and electrokinetic charge and titratable charges of the bare particles, in Figs. 1 and 3b.

The calculation in Eq. [4] indicates that in the unit cell at pH 6, 5.5 positive charges are lost from the interface as a result of adsorption, or on a per chain basis, 3.9 positive charges are lost per adsorbing chain. (The calculations on a per chain basis apply to the full range of coverage since the electrokinetic charge is linear in coverage in Fig. 3b). Since the cell initially contained two unbound cations inside the shear plane, it is likely that some loss of positive electrokinetic charge resulted from their release to a position beyond the shear plane. The other loss of positive charge could be a result of binding of additional $H_2PO_4^-$ counterions to the adsorbing polymer; however, this possibility is extremely unlikely, since it would involve a substantial loss of translation entropy. The other possibilities to explain the loss of positive interfacial charge are increased surface ionization as a result of adsorption, or decreased DMAEMA protonation, as a result of adsorption. We consider these two possibilities separately. First, it is possible that upon adsorption, the DMAEMA protonation decreases. A reduction in the DMAEMA protonation; however, would also imply a reduction in bound anionic counterions, since fewer $H_2PO_4^-$ counterions would be needed to preserve the Bjerrum length. While the release of these counterions would increase the entropy on adsorption, making the process more favorable, their release would counteract the loss of positive charge from the reduced backbone ionization. Therefore, a reduction in DMAEMA protonation would not explain the loss of positive charge on adsorption, unless the $H_2PO_4^-$ ions remained bound to the polymer, which seems unlikely. The possibility of DMAEMA protonation also seems unlikely because

on adsorption, the oligomer moves from a dilute to a relatively concentrated environment. Figure 1 illustrates, however, that increases in concentration are accompanied by an increase, not a decrease, in backbone protonation.

The ionization of the surface to release additional protons seems a more likely explanation of the loss of positive interfacial charge on adsorption. Presumably, the additional ionization occurring would do so in the vicinity of the adsorbing polymer, as illustrated in Fig. 4, to release 3.5 protons on average, in addition to the two undbound cations released to positions beyond the shear plane (46).

To summarize at pH 6, DMAEMA adsorption causes a net loss of 3.9 positive charges per chain from the interface. Of these, 1.4 are attributed to changes in the amount of unbound ions inside the shear plane, while the rest (2.5) result from an increased surface ionization in the vicinity of each adsorbed chain. This increase in the negative silica charge has been reported or speculated by other groups to cause additional polycation adsorption (1, 17). Here were agree that surface ionization does increase as a result of adsorption but the calculations of the previous section argue against its contribution as a driving force for further adsorption. Further, neglect of counterion condensation would have grossly overpredicted the surface ionization induced by polymer adsorption. The adsorbed amount correlates precisely with the titratable charge on the bare silica. The additional ionization merely contributes to the entropy increase on adsorption and possibly to the binding strength.

It is worth pointing out that the linearity of the electrokinetic charge and mobility traces over the full range of coverages suggests that these electrostatic features of adsorption (the changes in entrained ions and altered surface ionization) occur to the same extent for each adsorbing chain, consistent with the patchy adsorption concept. This means that our calculations based on the point of zero charge apply to the full range of coverages. Above the point of net surface neutralization, one might choose to think of the change in entrained ions as resulting from further entrainment of phosphates (as opposed to the loss of entrained sodiums and potassiums). Finally, one should note that the independence of ionization and bound counterion changes on coverage is consistent with the previously observed independence of adsorbed configuration on coverage (21). Each chain adsorbs at pH 6 in the same conformation, and the surface ionization increases to the same extent for each bound chain.

Table 2 summarizes similar calculations for all three pHs. It indicates that in the range from pH 6 to pH 8, when DMAEMA adsorbs, there is a net loss of positive charge, which diminishes as the pH is increased and which passes through a maximum on a per chain basis. Some of this loss of positive charge must necessarily result from loss of unbound cations inside the shear plane (when the surface has a net negative charge) or gain of unbound anions. Besides the change in free ions within the shear plane, additional positive charge is lost. This is best explained by surface ionization locally enhanced by DMAEMA adsorption, on the order of 2.5–2.7 negative surface charges generated beneath each adsorbed chain. This effect diminishes with increased pH.

TABLE 2
Adsorption-Induced Changes in Interfacial Charge

pH	$\Gamma_{\mu=0}$ (mg/m^2)	Δ Net charge (per chain)	Δ Entrained ions (per chain)	Δ Surface ionization (per chain)
6	0.22	−3.9	−1.4	−2.5
7	0.44	−4.2	−1.5	−2.7
8	0.62	−2.2	−2.2	0

SUMMARY

This work examined the charge-driven adsorption of DMAEMA on silica in the pH range from 6 to 8, where there was substantial adsorption and where the charge on the DMAEMA (including bound counterions) was more dense than that on the bare silica. Charge overcompensation was found under all conditions, though it was most pronounced at pH 6 where the polymer charge density most substantially exceeded that of the silica. As the pH was increased, the DMAEMA charge density decreased and that of the silica increased, leading to a reduction in the extent of charge overcompensation on the plateau of the isotherm. The charge overcompensation and the adsorbed mass on the isotherm plateau were explained quantitatively by the calculations whose essence is captured in Fig 5.

At pH 6, the surface charge is so sparse that one chain adsorbs on each surface charge and adsorbed chains are noninteracting. This scenario quantitatively explains the adsorbed mass on the plateau of the isotherm and is also consistent with a flat isotherm plateau. Additionally, the charge overcompensation at pH 6 results from the relatively large amount of positive charge brought

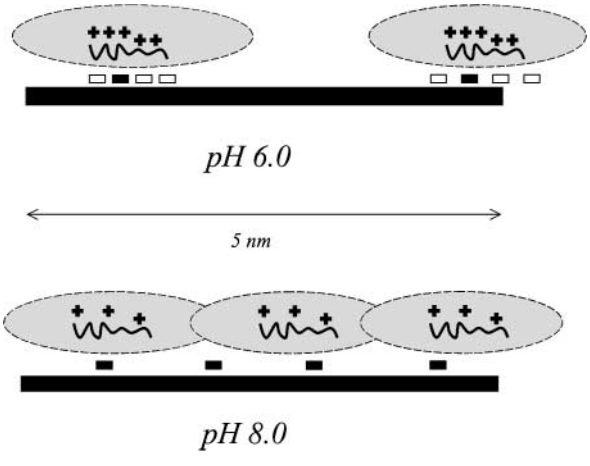

FIG. 5. Summary of transition from isolated chains with coverage limited by surface charge to interacting chains where excluded surface area limits the plateau coverage.

to the interface by adsorbing chains. Though the DMAEMA contains substantial positive charge, on adsorption, some of this positive charge is lost. Roughly 1.4 units of positive electrokinetic charge per chain are lost due to the release of free cations inside the shear plane or the gain of anions in the electrophoretic mobility experiment. More importantly, DMAEMA adsorption induces further silica ionization in the vicinity of the adsorbing oligomer with the release of about 2.5 protons and the generation of 2.5 new negative surface charges per adsorbing chain. The released protons contribute to the entropy of adsorption, while the additional negative surface charge interacts with the positive charge on the DMAEMA to enhance the adsorption energy. These effects occur to the same extent for each adsorbing chain, as indicated by the linearity of the electrokinetic mobility as a function of surface charge.

At higher pHs, the DMAEMA charge is reduced while the surface charge is increased, so that the system ultimately crosses over to a regime where coverage is limited, not by surface charge, but by the excluded surface area or repulsive interactions among adsorbing chains. Further, at pH 8, the adsorbing chains contain positive charges which are only slightly more dense than the underlying silica charge. Since the bare silica is already substantially ionized at pH 8, and the DMAEMA is relatively sparsely charged, its adsorption does not further increase the surface ionization.

This work has demonstrated, in addition to the crossover behavior for the adsorption of DMAEMA on silica, that ionization of the surface at the appropriate pH conditions is the main consequence of adsorption. Though our investigation is one of the few to quantitatively take counterion binding into account, we find no evidence for counterion release from the adsorbing chains. Incorporation of the counterions in the calculation is, however, essential to the correct estimation of surface ionization. Neglecting counterion binding would lead to a gross overestimate of the surface ionization induced on adsorption. Also, since there were few sodium and potassium ions chemically bound to the surface in the pH range of interest, cation release from the surface did not contribute to the driving force for adsorption.

ACKNOWLEDGMENTS

This work was supported by NSF Grants EEC9712915 and CTS 9817048, Lehigh's Polymer Interfaces Center. Mike Wolfe and Harry Spinelli of DuPont are acknowledged for their generous gift of the DMAEMA.

REFERENCES

1. Hoogeveen, N. G., Cohen Stuart, M. A., and Fleer, G. J., *J. Colloid Interface Sci.* **182,** 133 (1996).
2. Hoogeveen, N. G., Cohen Stuart, M. A., and Fleer, G. J., *J. Colloid Interface Sci.* **182,** 146 (1996).
3. Cosgrove, T., Obey, T. M., and Vincent, B., *J. Colloid Interface Sci.* **111,** 409 (1986).
4. Aksberg, R., Einarson, M., Berg, J., and Odberg, L., *Langmuir* **7,** 43 (1991).
5. Tanaka, H., and Odberg, L., *J. Colloid Interface Sci.* **149,** 40 (1992).
6. Wang, T. K., and Audebert, R., *J. Colloid Interface Sci.* **121,** 32 (1988).
7. Wang, T. K., and Audebert, R., *J. Colloid Interface Sci.* **119,** 459 (1987).
8. Durand-Piana, G., Lafuma, F., and Audebert, R., *J. Colloid Interface Sci.* **119,** 474 (1987).
9. Mabire, F. Audebert, R., and Quivoron, C., *J. Colloid Interface Sci.* **97,** 120 (1984).
10. Einarson, M., Aksberg, R., Odberg, L., and Berg, J. *Colloids Surf.* **53,** 183 (1991).
11. Tanaka, H., Odberg, L., Wagberg, L., and Lindstrom, T., *J. Colloid Interface Sci.* **134,** 219 (1990).
12. Eriksson, L., Alm, B., and Stenius, P. *Colloids Surf. A* **70,** 47 (1993).
13. Wiegel, F. W., *J. Phys. A* **10,** 299 (1997).
14. Muthukumar M., *J. Chem. Phys.* **86,** 7230 (1987).
15. Böhmer, M. R., Heesterbeek, W. H. A., Deratani, A., and Renard E., *Colloids Surf. A* **99,** 53 (1995).
16. van de Steeg, H. G. M., Cohen Stuart, M. A., Keizer, A., and Bijsterbosch, B. H., *Langmuir* **8,** 2538 (1992).
17. Sukhishvili, S. A., and Granick, S., *J. Chem. Phys.* **109,** 6861 (1998).
18. Bonekamp, B. C., and Lyklema, J., *J. Colloid Interface Sci.* **113,** 67 (1986).
19. Ferreira, M., Cheung, J. H., and Rubner, M. F., *Thin Solid Films* **244,** 806 (1994).
20. Bohmer, M. R., Evers, O. A., and Scheutjens, J. M. H. M., *Macromolecules* **23,** 2288 (1990).
21. Shin, Y., Roberts, J. E., and Santore, M. M., *J. Colloid Interface Sci.* **244,** 190 (2001).
22. Popping, B., Seville, B., Deratani, A., Desbois, N., Lamarche, J. M., and Boissy, A., *Colloids Surf.* **64,** 125 (1994).
23. Williams, P. A., Harrop, R., Phillips, G. O., Pass, G., and Robb, I. D., *J. Chem. Soc. Faraday Trans I* **78,** 1733 (1982).
24. Durand, G., Lafauma, F., and Audebert, R., *Prog. Colloid Polym. Sci.* **266,** 278 (1988).
25. Danlgren, M. A. G., *Langmuir* **10,** 1580 (1994).
26. Shin, Y., Santore, M. M., and Roberts, J. E., submitted for publication.
27. van Leeuwen, H. P., Cleven, R. F. M. J., and Valenta, P., *Pure Appl. Chem.* **63,** 1251 (1991).
28. Vink, H., J. *Chem. Soc. Faraday Trans. I* **85,** 699 (1989).
29. Papenhuijzen, J., Van der Schee, H. A., and Fleer, G. J., *J. Colloid Interface Sci.* **104,** 540 (1985).
30. Shin, Y., Ph.D. dissertation, Lehigh University, 2002.
31. Park, S., Barrett, C. J., Rubner, M. F., and Mayes, A. *Macromolecules* **34,** 3384 (2001).
32. Martin, M. L., Delpuech, J.-J., and Martin, G. J., "Practical NMR Spectroscopy," Heyden, London, 1980.
33. Manning, G. S., *J. Chem. Phys.* **51,** 924 (1969).
34. Manning, G. S., *J. Chem. Phys.* **51,** 934 (1969).
35. Bousse, L., De Rooij, N. F., and Bergveld, P., *Surface Science,* **135,** 479 (1983).
36. Bergveld, P., and Sibbald, A., *in* "Wilson and Wilson's Comprehensive Analytical Chemistry" (G. Svehla, Ed.), Vol XXIII, pp. 21–37, Elsevier, New York, 1988.
37. Shin, Y., Ph.D. thesis, Lehigh University, 2002.
38. Fung, C. D., Cheung, P. W., and Ko, W. H., *IEEE Trans. Electron Devices* **ED-33,** 8 (1986).
39. Hunter, R. J., "Zeta Potential in Colloidal Science," pp. 100–112, Academic Press, London, 1981.
40. Ottewill, R. H., and Shaw, J. N., *J. Electroanal. Chem.* **37,** 133 (1972).
41. O'Brien, R. W., and White, L. R., *J. Chem. Soc. Faraday Trans. II* **74,** 1607 (1978).
42. Garvey, M. J., Tadros, Th. F., and Vincent, B. *J. Colloid Interface Sci.* **55,** 440–453 (1976).
43. Note: At pH 6 the dominant phosphate ion is $H_2PO_4^-$, but at pH 8 it is $HPO_4^=$. In this work, we are more concerned with counting the charge

contained by these ions, rather than the actual numbers or identities of the particular phosphate ions condensing on the DMAEMA. In some situations, this may be an important distinction; however, in the current work it is a minor detail. Further in the titration curves for Fig. 1, the counterions on the DMAEMA were chlorines, as HCl was added at the beginning of each titration to fully protonate the DMAEMA amines.

44. Perram, J. W., Hunter, R. J., and Wright, H. J. L., *Aust. J. Chem.* **27,** 461 (1974).
45. Yates, D. E., Levine, S., and Healy, T. W., *J. Chem. Soc. Faraday Trans I* **70,** 1807 (1974).
46. While 3.5 protons must be released as a result of additional surface ionization in the vicinity of adsorbed chains, it is also possible that the surface ionizes even more, in a "second process." For surface ionization grater than 3.5 sites/bound cell, in addition to the released protons, negative counterions must also be released from the polymer. This second process might in principle be detected through conductimetric titrations; however, due to the already large amounts of ions present, it was impossible to detect. The extent to which the second process occurs depends on how interfacial conditions (different dielectric constants one either side of a half-space) affect the Bjerrum length.